# Analytical study of the post-closure behaviour of a deep tunnel in a porous creeping rock mass

Frédéric Deleruyelle [a], Tuan Anh Bui [b,*], Henry Wong [b], Nathalie Dufour [c],
Duc Kien Tran [d], X.S. Zhang [e]

[a] *IRSN/PRP-DGE/SEDRAN/B4S, Fontenay-aux-Roses, France*
[b] *Université de Lyon, ENTPE/LGCB and LTDS UMR CNRS 5513, Vaulx-en-Velin, France*
[c] *CEREMA – DTerMed, Aix-en-Provence, France*
[d] *Université de Lyon, ECL/LTDS UMR CNRS 5513, Écully, France*
[e] *Institute of Resources and Environment, North China University of Water Resources and Electric Power, Zhengzhou, China*

A B S T R A C T

The deferred behaviour of underground cavities is often encountered in geotechnical engineering. This paper presents an analytical approach for the post-closure behaviour of a deep tunnel inside a rock mass considering both creep and hydromechanical couplings. Creep, supposed slower than hydraulic flow, is described by a linear Norton–Hoff law in the particular case of an elastically incompressible rock mass (i.e. Poisson's ratio $\nu = 0.5$). The resolution uses Laplace transform and Stehfest's algorithm. Numerical examples are carried out to enlighten the hydromechanical responses around the tunnel and to show the consistency of the solution.

© 2016 Académie des sciences. Published by Elsevier Masson SAS. This is an open access article under the CC BY-NC-ND license (http://creativecommons.org/licenses/by-nc-nd/4.0/).

## 1. Introduction

The time-dependent behaviour of deep cavities must often be properly accounted for in geotechnical engineering, such as mining industry [1], oil and gas extraction [2,3], and radioactive waste disposal design [4,5]. A number of previous works have studied this important issue, but most of them require advanced numerical tools and sophisticated modelling [6–8] to take into account the exact geometry and the different sequences of achievement of the structure as well as the complexity of the mechanical behaviours. Therefore, these numerical results are generally difficult to interpret and not easy to check due, among others, to the very long time scale considered as in a post-closure issue.

Thus, some analytical modelling has also been performed [4,9,10] to provide reliable solutions in some limiting cases. They also constitute useful benchmarks for numerical solutions and improve the physical understanding of the involved phenomena. However, very few analytical models take into account the effect of creep and hydromechanical (HM) coupling in the rock mass, although it has been experimentally evidenced [11–13], and despite its important role for the evaluation of structural performance, for instance, the long-term safety assessment of a radioactive waste-disposal facility [14–16].

This paper aims at studying analytically the post-closure behaviour of a typical tunnel inside a rock mass with regards to both creep and HM coupling. It is a direct continuation of the work by Deleruyelle et al. [17] for post-closure stages. HM modelling relies on the basis of poromechanics [18], while creep is described by the Norton–Hoff law. Similar to [17], only
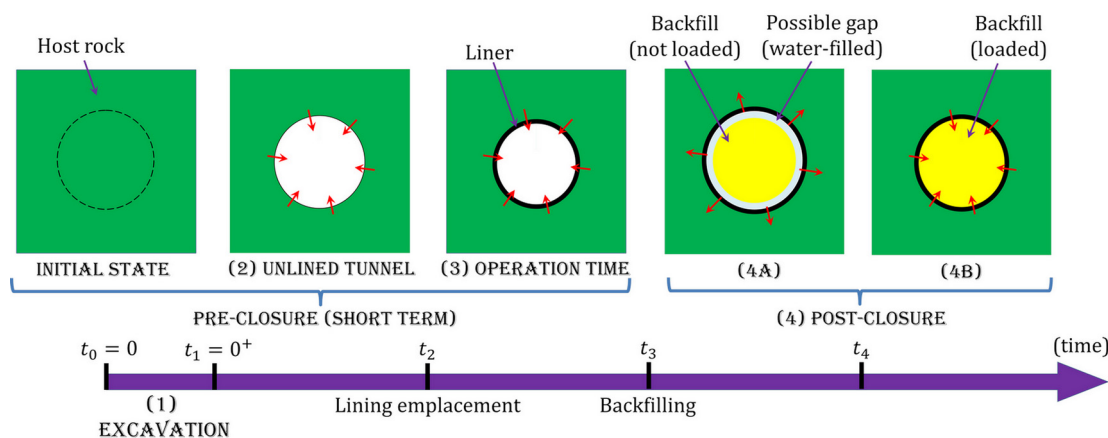
**Fig. 1.** Simplified life cycle of a typical tunnel. Red arrows show the movement of the rock mass: convergence (inward arrows) or divergence (outward arrows). Green colour: host rock, yellow colour: backfill.

the particular case of an elastically incompressible rock mass (i.e. Poisson's ratio $\nu = 0.5$) obeying a "linear" version of this creep law (see Eq. (8) below) is considered. An additional assumption is that creep effects are much slower than hydraulic flow. The resolution is performed using Laplace transform and Stehfest's inversion algorithm [19]. Finally, some numerical applications are performed to enlighten the HM responses of the cavity and to show the consistency of the solution.

## 2. General framework

### 2.1. Post-closure issue in porous viscoplastic media

The tunnel life cycle is idealized as four stages schematized in Fig. 1. Initially, at $t = t_0 = 0$, the surrounding rock is supposed to be in equilibrium with the hydrostatic pressure $p_{w0}$ and the geostatic pressure $P_\infty$. The first stage corresponds to the excavation of a circular tunnel of radius $a$ in an infinite, isotropic, and homogeneous poro-viscoplastic medium characterized by a Young modulus $E$, a Poisson ratio $\nu$, a rock viscosity $\eta$, and a hydraulic conductivity $\lambda_h$. The time required for excavation is supposed small compared to the characteristic creep time so that excavation can be considered as instantaneous and ends at $t = t_1 = 0^+$. It is followed by the second stage, during which the unlined tunnel exhibits some convergence. This stage ends when a lining support is emplaced at $t = t_2$, marking the beginning of Stage 3. The hydraulic conductivity of this liner is supposed to be much higher than that of the surrounding rock. During Stages 2 and 3, water seeping from the medium is assumed to be removed so that at the tunnel wall, groundwater remains at atmospheric pressure.

The above three stages (pre-closure) are followed by the fourth and last one, called post-closure stage, and starting from $t = t_3$ when the tunnel is backfilled. During this stage, the tunnel is no longer open and the water seeping from the cavity wall slowly restores its natural pressure. Depending on the kinetics of creep and hydraulic flow, the cavity wall can continue its converging movement or exhibit a divergent one. In the following, the assumption is made that (i) the creep effect is much slower than the hydraulic flow and (ii) the lining remains in close contact with the cavity wall. Under these conditions, as a first step, the cavity wall moves outward from the tunnel axis as water pressure in the cavity increases (which opposes to the creep effect), while the backfill remains immobile and unloaded (Stage 4A). After a large time, the hydraulic balancing stabilizes and the cavity wall can resume a converging movement. If this re-convergence is significant enough, the rock and the liner can compress the backfill from a time $t_4 > t_3$, which marks the end of Stage 4A and the beginning of Stage 4B. Otherwise, the backfill will never be loaded and Stage 4B never occurs.

### 2.2. Main equations

In cylindrical coordinates, the usual conditions of *axisymmetry* and *plane strains* lead to diagonal stress $\boldsymbol{\sigma}$ and strain $\boldsymbol{\varepsilon}$ tensors and a purely radial displacement field $\boldsymbol{u}$:

$$\boldsymbol{\sigma} = \begin{bmatrix} \sigma_r & & \\ & \sigma_\theta & \\ & & \sigma_z \end{bmatrix}; \qquad \boldsymbol{u} = \begin{pmatrix} u \\ 0 \\ 0 \end{pmatrix}; \qquad \boldsymbol{\varepsilon} = \begin{bmatrix} \frac{\partial u}{\partial r} & & \\ & \frac{u}{r} & \\ & & 0 \end{bmatrix}; \qquad U(t) \equiv \frac{u(a,t)}{a} \tag{1}$$

In the above, $U(t)$ is defined as the relative convergence at the tunnel wall. The volumetric strain $\epsilon$ is linked to the only non-null component of displacement $u$ by:

$$\epsilon = \text{tr}(\boldsymbol{\varepsilon}) = \frac{\partial u}{\partial r} + \frac{u}{r} \tag{2}$$

The equilibrium equation writes, in cylindrical coordinates:

$$r\frac{\partial \sigma_r}{\partial r} + \sigma_r - \sigma_\theta = 0 \tag{3}$$

The strain tensor $\boldsymbol{\varepsilon}$ and variation of porosity $(\phi - \phi_0)$ can be partitioned into elastic and viscoplastic parts, marked by superscripts $^e$ and $^{vp}$, respectively:

$$\boldsymbol{\varepsilon} = \boldsymbol{\varepsilon}^e + \boldsymbol{\varepsilon}^{vp}; \qquad \phi - \phi_0 = \phi^e + \phi^{vp} \tag{4}$$

The elastic parts are described by the classic poroelastic equations [18]:

$$\dot{\boldsymbol{\varepsilon}}^e = \frac{1}{3K}\dot{\sigma}'_m \mathbf{1} + \frac{1}{2G}\dot{\boldsymbol{s}} \tag{5}$$

$$\dot{\phi}^e = b\dot{\epsilon}^e + \beta \dot{p}_w \tag{6}$$

where $\mathbf{1}$ stands for the second-order identity tensor; $b = 1 - K/K_s$ is Biot's coefficient; $\beta = (b - \phi_0)/K_s$ is the pore compressibility ($K_s$: the bulk modulus of the solid phase); $\sigma'_m = \text{tr}(\boldsymbol{\sigma}')/3 = \sigma_m + bp_w$ is the mean effective stress ($\boldsymbol{\sigma}' = \boldsymbol{\sigma} + bp_w\mathbf{1}$: effective stress tensor; $\sigma_m = \text{tr}(\boldsymbol{\sigma})/3$: mean total stress); $\boldsymbol{s} = \boldsymbol{\sigma} - \sigma_m\mathbf{1}$ is the deviatoric stress tensor; $K = E/[3(1 - 2\nu)]$ and $G = E/[2(1 + \nu)]$ are the drained bulk and shear moduli.

For the viscoplastic parts, we adopt the following assumption [18]:

$$\phi^{vp} = b\epsilon^{vp} \tag{7}$$

where $\epsilon^{vp}$ is the viscoplastic volumetric strain. Based on the thermodynamic approach [20], the viscoplastic strain rate is thermodynamically derived from a dissipation potential, assumed to depend solely on the effective stress tensor $\boldsymbol{\sigma}' = \boldsymbol{\sigma} + bp_w$ and to obey a Norton–Hoff creep law $\varphi^* = q^{n+1}/[(n+1)\eta]$ where $q = \sqrt{(3/2)\boldsymbol{s}:\boldsymbol{s}}$ is the Von Mises equivalent stress and $n$ a stress exponent. The viscoplastic strain rate is then given by:

$$\dot{\boldsymbol{\varepsilon}}^{vp} = \frac{\partial \varphi^*}{\partial \boldsymbol{\sigma}'} = \frac{3q^{n-1}}{2\eta}\boldsymbol{s} \tag{8}$$

Moreover, combining assumption (7), equation (6), the mass balance equation of the fluid phase and the Darcy law, the following diffusion equation is obtained:

$$b\dot{\epsilon} = -\frac{1}{M}\dot{p}_w + \lambda_h \Delta p_w \tag{9}$$

where $M$ denotes Biot's modulus (defined by $1/M = \beta + \phi_0/K_w$), $K_w$ the bulk modulus of the fluid phase and $\Delta = \nabla \cdot \nabla$ the Laplace operator.

Furthermore, it is assumed that in the far field, displacements and pore pressures are never affected. The boundary conditions at infinity are therefore always expressed as follows:

$$u(\infty, t) = 0; \qquad p_w(\infty, t) = p_{w0} \tag{10}$$

By contrast, the boundary conditions at the tunnel wall differ at each stage and will be specified later.

## 3. Analytical resolution for a particular case of porous media

### 3.1. Existing analytical solution for the pre-closure behaviour

Due to the high complexity of the post-closure behaviour, a fully coupled HM behaviour seems to be very complicated to solve. To simplify, we only focus on the particular case where the rock Poisson's ratio $\nu = 0.5$ (elastic incompressibility) and the stress exponent $n = 1$. In this case, Eqs. (5) and (8) become:

$$\dot{\boldsymbol{\varepsilon}}^e = \frac{1}{2G}\dot{\boldsymbol{s}} \tag{11}$$

$$\dot{\boldsymbol{\varepsilon}}^{vp} = \frac{3}{2\eta}\boldsymbol{s} \tag{12}$$

which leads to $\dot{\epsilon} = \dot{\epsilon}^e = \dot{\epsilon}^{vp} = 0$, which means that neither elastic nor creep strains induce any volume change. This, in consequence, combining with (2) and (10), leads to:

$$u(r, t) = U(t)\frac{a^2}{r} \tag{13}$$

Additionally, the diffusion equation (9) is simplified to:

$$-\dot{p}_w + M\lambda_h \Delta p_w = 0 \tag{14}$$

**Table 1**
Main results for the first three stages [17].

| | Stage 1 $(0 \le t \le 0^+)$ | Stage 2 $(0^+ \le t \le t_2)$ | Stage 3 $t_2 \le t \le t_3$ |
|---|---|---|---|
| Displacement | $u = -\frac{a^2}{r}\frac{P_\infty}{2G}$ | $u = -\frac{a^2}{r}\frac{P_\infty}{2G}\left(1 + \frac{t}{T_0}\right)$ | $u = -\frac{a^2}{r}\left[\frac{P_\infty}{2G}\left(1 + \frac{t_2}{T_0}\right) + \frac{P_\infty}{K_L}\left(1 - e^{-\frac{t-t_2}{T_2}}\right)\right]$ |
| Pore pressure | $p_w = p_{w0}$ | $\overline{p_w}(r,s) = \frac{p_{w0}}{s}\left[1 - \frac{K_0[\Omega(s)r]}{K_0[\Omega(s)a]}\right]$ | $\overline{p_w}(r,s) = \frac{p_{w0}}{s}\left[1 - \frac{K_0[\Omega(s)r]}{K_0[\Omega(s)a]}\right]$ |

It is observed that under the simplifying assumptions, the HM behaviour only remains coupled through the boundary conditions at the gallery wall. This case remains however interesting and the stress exponent assumption, albeit strong, can also be met for instance in [13]. On account of the above equations, semi-analytical solutions have been addressed for the first three stages [17,21] and are shortly recalled hereafter in Table 1.

In this table, $\overline{f}(r,s)$ denotes the Laplace transformed function of $f(r,t)$, defined by $\overline{f} = \mathcal{L}(f) = \int_0^\infty f(r,t)e^{-st}dt$; $I_0$ and $K_0$ are the zeroth-order modified Bessel functions of the first and second kind; $\Omega(s) = \sqrt{s/(\lambda_h M)}$; $T_0 = \eta/(3G)$ is a characteristic relaxation time; and $T_2 = (1 + 2G/K_L)T_0$ is a characteristic time accounting for the presence of a lining that provides an elastic radial support pressure $p_L(t)$ written as:

$$p_L(t) = -K_L[U(t) - U_2]; \quad U_2 = U(t_2) \tag{15}$$

where $K_L$ is the stiffness of the lining. Note that mechanical fields are expressed explicitly in the real-time domain, while hydraulic fields (pore pressures) are only addressed in the Laplace transform domain. To obtain the solution in the real-time domain, a numerical inversion by Stehfest's algorithm [19], whose validity has been previously verified [10,17,21], is applied:

$$f(r,t) = \mathcal{L}^{-1}\left[\overline{f}(r,s)\right] \cong \frac{\ln 2}{t}\sum_{n=1}^{\mathcal{N}} C_n \overline{f}\left(r, n\frac{\ln 2}{t}\right)$$

$$C_n = (-1)^{n+\frac{\mathcal{N}}{2}} \sum_{k=\text{Int}(\frac{n+1}{2})}^{\min(n,\frac{\mathcal{N}}{2})} \frac{k^{\frac{\mathcal{N}}{2}}(2k)!}{(\frac{\mathcal{N}}{2}-k)!k!(k-1)!(n-k)!(2k-n)!} \tag{16}$$

where $\text{Int}(x)$ means the integer part of $x$, and $\mathcal{N}$ is an even positive integer. In the following, we will now extend these results to the post-closure stage.

### 3.2. Semi-analytical resolution for Stage 4A

The initial conditions for this stage are taken from the results of Stage 3 at $t = t_3$. While the solutions for mechanical fields are totally explicit, only approximate solutions provided by Stehfest's formula (16) are available for hydraulic fields (see Table 1). Since the coefficients $C_n$ defined by (16) satisfy $\sum_{n=1}^{\mathcal{N}} \frac{C_n}{n} \equiv 1$ for any even positive integer $\mathcal{N}$, the initial condition for the pore pressure writes:

$$p_{w3}(r) = p_w(r, t_3) \approx p_{w0}\left[1 - \sum_{n=1}^{\mathcal{N}} \frac{C_n}{n}\frac{K_0(\Omega_n r)}{K_0(\Omega_n a)}\right]; \quad \Omega_n = \Omega(s_n); \quad s_n = \frac{n \cdot \ln 2}{t_3} \tag{17}$$

At this stage, the backfill has to be considered. It is modelled as a cylinder of radius $a$ made of an initially zero-stress, poroelastic, and fully saturated material. Its permeability is supposed much higher than that of the rock mass so that its pore pressure is homogeneous. Furthermore, we assume that its solid phase is incompressible. Such a configuration has been analysed in [10]. The incremental relation between effective stress and displacement at the external wall of the backfill (denoted by $a^-$) writes:

$$\dot{\sigma}_r'(a^-, t) = \dot{\sigma}_r(a^-, t) + \dot{p}_w(a^-, t) = K_R \frac{\dot{u}(a^-, t)}{a} \tag{18}$$

where $K_R = 2(K' + G'/3)$ is the stiffness of the backfill, with $K'$ and $G'$ are its bulk and shear moduli.

According to previous assumptions (§ 2.1), the lining moves outward from the tunnel during this stage, at $r = a^-$ a total stress variation $d\sigma_r(a^-, t)$ is induced by an increase of water pressure $dp_w = -d\sigma_r$, thus the backfill is immobile, $du(a^-, t) = 0$. Hence, a separation between the lining and backfill occurs and the latter has no mechanical effect on the rock mass. The mechanical boundary condition for the rock mass at the tunnel wall $r = a^+$ writes:

$$\sigma_r(a^+, t) = -p_L(t) - p_w(a^+, t) \tag{19}$$

where $p_L(t)$ is given by (15). Using the results obtained in Appendix A, Eq. (19) can be rewritten in terms of displacement and pore pressure fields as follows:

$$\dot{U}(t) + \frac{1}{T_2}U(t) = \frac{K_L U_2 + p_w(a,t) - P_\infty}{K_L T_2} + \frac{\dot{p}_w(a,t)}{K_L + 2G} \tag{20}$$

Assuming that the solid phase of the backfill and the lining are incompressible, one can conclude that a volume change of the tunnel, governed by the rate of rock mass convergence, corresponds to an identical volume of water in the tunnel. The latter includes a volume of water influx or outflux, governed by Darcy's law, and a volumetric contraction of water due to water pressure increase. Consequently, the hydraulic boundary condition at the tunnel wall writes:

$$\lambda_h \frac{\partial p_w}{\partial r}(a^+, t) - \phi_0 \frac{a}{3}\frac{\dot{p}_w(a,t)}{K_w} = a\dot{U}(t) \tag{21}$$

Denoting $\tau = (t - t_3)$, the following *translated* fields are defined: $\hat{p}_w(r, \tau) = p_w(r, t); \hat{U}(\tau) = U(t)$. Applying this translation, then the Laplace transform on (20) and (21), and taking into account the initial conditions at $\tau = 0$ (i.e. $t = t_3$), we get:

$$\overline{\hat{U}}(s) = M(s)\overline{\hat{p}_w}(a,s) + N(s) \tag{22}$$

$$\lambda_h \frac{\partial \overline{\hat{p}_w}}{\partial r}(a,s) = as\left(M(s) + \frac{\phi_0}{3K_w}\right)\overline{\hat{p}_w}(a,s) + asN(s) - aU_3; \quad U_3 = U(t_3) \tag{23}$$

where:

$$M(s) = \left(\frac{1}{K_L T_2} + \frac{s}{K_L + 2G}\right)\left(s + \frac{1}{T_2}\right)^{-1}; \qquad N(s) = \left[U_3 + \frac{K_L U_2 - P_\infty}{K_L T_2 \cdot s}\right]\left(s + \frac{1}{T_2}\right)^{-1} \tag{24}$$

Applying then the Laplace transform to the diffusion equation (9), we obtain:

$$\frac{\partial^2 \overline{\hat{p}_w}(r,s)}{\partial r^2} + \frac{1}{r}\frac{\partial \overline{\hat{p}_w}(r,s)}{\partial r} - \Omega^2(s)\overline{\hat{p}_w}(r,s) = -\frac{\Omega^2(s)}{s}p_{w3}(r) \tag{25}$$

Using (17), Eq. (25) gives the following solution for the pore pressure:

$$\overline{\hat{p}_w}(r,s) = A(s)K_0\big[\Omega(s)r\big] + B(s)I_0\big[\Omega(s)r\big] + p_{w0}\left(\frac{1}{s} - \sum_{n=1}^{\mathcal{N}}\frac{C_n t_3}{n(st_3 - n\ln 2)}\frac{K_0(\Omega_n r)}{K_0(\Omega_n a)}\right) \tag{26}$$

where $A(s)$ and $B(s)$ are constants of integration. Accounting for the boundary conditions (10) and (23) and noting that $\lim_{x\to\infty} I_0(x) = \infty; \lim_{x\to\infty} K_0(x) = 0$, we deduce $B(s) = 0$ while $A(s)$ is calculated as:

$$A(s) = \left[\lambda_h p_{w0}\sum_{n=1}^{\mathcal{N}}\frac{C_n t_3 \Omega_n}{n(st_3 - n\ln 2)}\frac{K_1(\Omega_n a)}{K_0(\Omega_n a)} - as\left(M(s) + \frac{\phi_0}{3K_w}\right)p_{w0}\left(\frac{1}{s} - \sum_{n=1}^{\mathcal{N}}\frac{C_n t_3}{n(st_3 - n\ln 2)}\right)\right.$$

$$\left. - asN(s) + aU_3\right]\left[\lambda_h\Omega(s)K_1\big[\Omega(s)a\big] + as\left(M(s) + \frac{\phi_0}{3K_w}\right)K_0\big[\Omega(s)a\big]\right]^{-1} \tag{27}$$

where $K_1$ is the first-order modified Bessel function of second kind. From (27), (26) and (22), the pore pressure and displacement fields are totally defined in the Laplace domain. The solution in the time domain is then assessed using Stehfest's algorithm (16).

### 3.3. Semi-analytical resolution for Stage 4B

This stage takes place if for large time values (§ 2.1), the rock mass and the lining resume a converging movement and compress the backfill. Since the backfill is immobile during the previous stage, the time $t_4$ that indicates the onset of this stage corresponds to an initial value $U(t_4) = U_3$. Knowing the approximate form of the function $U(t)$ during Stage 4A, the value $t_4$ can be numerically calculated with a root-finding algorithm.

A numerical approximation of the initial pore pressure profile for this stage can be calculated from (26), (27) and (16):

$$p_w(r, t_4) \approx p_{w0} + \frac{\ln 2}{t_4 - t_3}\sum_{n=1}^{\mathcal{N}'}C_n A(s_n')K_0(\Omega_n' r) + p_{w0}\sum_{k=1}^{\mathcal{N}}D_k K_0(\Omega_k r) \tag{28}$$

$$D_k = -\sum_{n=1}^{\mathcal{N}'}C_n\frac{\ln 2}{t_4 - t_3}\frac{C_k t_3}{k(s_n' t_3 - k\ln 2)K_0(\Omega_k a)}; \quad s_n' = \frac{n \cdot \ln 2}{t_4 - t_3}; \qquad \Omega_n' = \Omega(s_n') \tag{29}$$

Due to the interaction between the lining and backfill, the boundary condition (19) becomes:

$$\sigma_r(a,t) = -p_L(t) - p_R(t) - p_w(a,t) \tag{30}$$

where $p_R(t)$ is the effective pressure at the outer boundary of the backfill, calculated using (18):

$$p_R(t) = -K_R\big[U(t) - U_3\big] \tag{31}$$

By the same procedure as in Appendix A, Eq. (30) can be reformulated as follows:

$$\dot{U}(t) + \frac{1}{T_3}U(t) = \frac{K_L U_2 + K_R U_3 - P_\infty + p_w(a,t)}{(K_L + K_R)T_3} + \frac{\dot{p_w}(a,t)}{K_L + K_R + 2G} \tag{32}$$

where the characteristic time $T_3$ is defined as $T_3 = (K_L + K_R + 2G)T_0/(K_L + K_R)$. One can realize that (32) will be simplified to (20) if $K_R = 0$, which interprets the case where the backfill has no mechanical effect on the rock mass and the lining support. Moreover, if the hydraulic effect is neglected, we obtain the results presented in Appendix B, which deals with the case of a tunnel in a dry ground, even when the host rock is compressible ($\nu \neq 0.5$).

The hydraulic boundary condition (21) is still valid for this Stage 4B. Similar to the previous one (42), the system of boundary equations (32) and (21) will be written in the Laplace transform domain. First, a translation is applied to the relative convergence and pore pressure: $\hat{p}_w'(r,\tau') = p_w(r,t)$; $\hat{U}'(\tau') = U(t)$ where $\tau' = (t - t_4) \in [0, \infty)$. Then, the Laplace transform applies to (32) and (21), and we get:

$$\overline{\hat{U}'}(s) = \overline{\hat{p}_w'}(a,s)M'(s) + N'(s) \tag{33}$$

$$\lambda_h \frac{\partial \overline{\hat{p}_w'}}{\partial r}(a,s) = as\left(M'(s) + \frac{\phi_0}{3K_w}\right)\overline{\hat{p}_w'}(a,s) + asN'(s) - aU_3 - \frac{a\phi_0}{3K_w}p_{w4}(a) \tag{34}$$

where:

$$M'(s) = \left(\frac{1}{(K_L + K_R)T_3} + \frac{s}{K_L + K_R + 2G}\right)\left(s + \frac{1}{T_3}\right)^{-1}$$

$$N'(s) = \left[U_3 + \frac{K_L U_2 + K_R U_3 - P_\infty}{(K_L + K_R)T_3 \cdot s} - \frac{p_{w4}(a)}{K_L + K_R + 2G}\right]\left(s + \frac{1}{T_3}\right)^{-1} \tag{35}$$

Similar to that at the previous stage (42), the diffusion equation (9) is written in the Laplace domain as follows:

$$\frac{\partial^2 \overline{\hat{p}_w'}(r,s)}{\partial r^2} + \frac{1}{r}\frac{\partial \overline{\hat{p}_w'}(r,s)}{\partial r} - \Omega^2(s)\overline{\hat{p}_w'}(r,s) = -\frac{\Omega^2(s)}{s}p_{w4}(r); \qquad p_{w4}(r) = p_w(r, t_4) \tag{36}$$

Invoking (28), the general solution of (36) writes:

$$\overline{\hat{p}_w'}(r,s) = A'(s)K_0\big[\Omega(s)r\big] + B'(s)I_0\big[\Omega(s)r\big] + \frac{p_{w0}}{s} + \sum_{n=1}^{\mathcal{N}'}\frac{C_n A(s_n')}{s - s_n'}\frac{\ln 2}{t_4 - t_3}K_0\big(\Omega_n'r\big) + p_{w0}\sum_{k=1}^{\mathcal{N}}\frac{D_k}{s - s_k}K_0(\Omega_k r) \tag{37}$$

By the same reasoning as for Stage 4A, we deduce that $B'(s) = 0$, while $A'(s)$ is:

$$A'(s) = -\left[\sum_{n=1}^{\mathcal{N}'}\frac{C_n A(s_n')}{s - s_n'}\frac{\ln 2}{t_4 - t_3}\left[\lambda_h\Omega_n'K_1\big(\Omega_n'a\big) + as\left(M'(s) + \frac{\phi_0}{3K_w}\right)K_0\big(\Omega_n'a\big)\right] + p_{w0}a\left(M'(s) + \frac{\phi_0}{3K_w}\right)\right.$$

$$+ \sum_{k=1}^{\mathcal{N}}\frac{p_{w0}D_k}{s - s_k}\left[\lambda_h\Omega_k K_1(\Omega_k a) + as\left(M'(s) + \frac{\phi_0}{3K_w}\right)K_0(\Omega_k a)\right] + asN'(s) - aU_3$$

$$\left. - \frac{a\phi_0}{3K_w}p_{w4}(a)\right]\left[\lambda_h\Omega(s)K_1\big[\Omega(s)a\big] + as\left(M'(s) + \frac{\phi_0}{3K_w}\right)K_0\big[\Omega(s)a\big]\right]^{-1} \tag{38}$$

The transformed pore pressure and displacement fields are totally defined by (37), (38), and (33). The solution in the real-time domain is obtained by means of Stehfest's algorithm described earlier.

## 4. Numerical applications

In this section, the analytical solutions presented above are applied to study the HM evolutions in the vicinity of a circular tunnel. The data concerning the cavity and the rock mass are suggested by [13,22,23], which are relative to a deep geological disposal facility for radioactive waste studied in France, and referred to in the following as "reference parameters" (see Table 2). Concerning the rock mass viscosity, $\eta_0$ in the order of $10^{17}$ Pa·s is a particularly low value for sound argillite, observed on some laboratory tests, but maybe due to damage effects or shortness of the tests, and considered here as a lower value in order to emphasize creep effects. The mechanical properties of the lining (made of concrete) are taken from [24,25]. It should be noted that the Biot coefficient is taken as $b = 0.6$, leading to $K/K_s = 0.4$, which does not contradicts the assumption of elastic incompressibility ($\nu = 0.5$ hence $K \longrightarrow \infty$) made in Section 2.

**Table 2**

Reference parameters used in numerical applications.

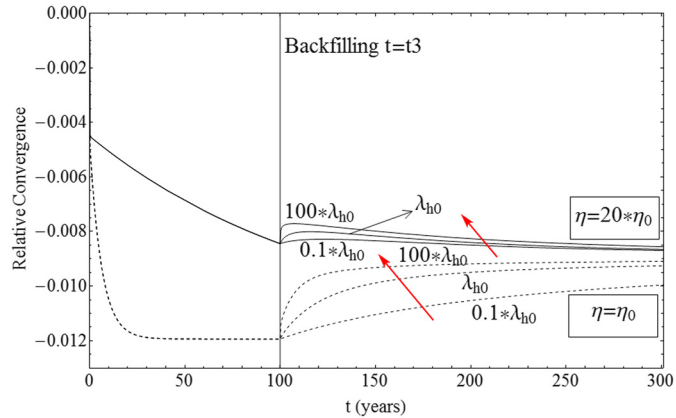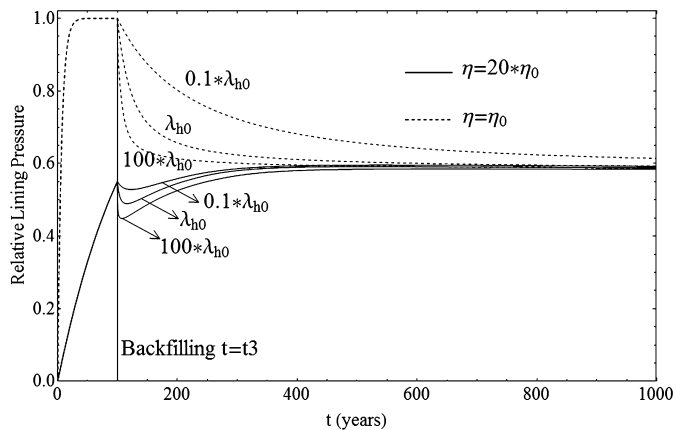| |
|---|
| $a = 5.0$ m; $e = 0.5$ m; $P_\infty = 12$ MPa; $p_{w0} = 5$ MPa; |
| $E = 4000$ MPa; $\eta_0 = 3.0 \cdot 10^{17}$ Pa·s; $E_L = 15000$ MPa; $\nu_L = 0.2$; $K_r = 192$ MPa; $K_L = 1684$ MPa; |
| $\lambda_h = 10^{-16}$ m$^4$·N$^{-1}$·s$^{-1}$; $b = 0.6$; $K_w = 2200$ MPa; $\phi_0 = 0.15$; |
| $t_0 = 0$; $t_1 = 0^+$; $t_2 = 2$ months; $t_3 = 100$ years |



**Fig. 2.** Temporal evolution of relative convergence with different hydraulic conductivities (continuous lines: $\eta = 20\eta_0$; dashed lines: $\eta = \eta_0$).



**Fig. 3.** Temporal evolution of relative lining pressure with different hydraulic conductivities (continuous lines: $\eta = 20\eta_0$; dashed lines: $\eta = \eta_0$).

Fig. 2 shows that with a lower value of rock viscosity $\eta = \eta_0$ (dashed lines), rock creep is already stabilized before backfilling occurs; thus, during the post-closure stage, only a divergent movement of the tunnel wall is observed (i.e. only Stage 4A occurs). On the contrary, if the rock mass viscosity is higher ($\eta = 20\eta_0$, continuous lines), the rock mass still has the potential to creep after the backfill emplacement. Consequently, after a first period of outward movement due to hydraulic restoration, creep effects override and resume a converging movement afterward. In any case, an increase of the permeability accelerates the movement of the tunnel wall.

Fig. 3 shows that the evolution of the movement at the tunnel wall is consistent with the evolution of the relative lining pressure (real value divided by the overburden). For a low viscosity (dashed lines), the lining pressure reaches the geostatic value before backfilling and monotonically decreases afterward towards an asymptotic value, with a rate enhanced by permeability. Since the backfill is never loaded, the asymptotic lining pressure at large times corresponds to the difference between the geostatic pressure and the initial hydrostatic water pressure. For a higher viscosity, the lining pressure is still increasing when backfilling occurs and remains substantially lower than the overburden. It decreases a little immediately after the emplacement of the backfill, due to the divergence of the tunnel wall, but then resumes and tends to the same asymptotic value as in the previous case.

As indicated in Fig. 4, during this post-closure stage, water pressure increases at the tunnel wall from its zero initial value. Moreover, the higher the permeability is, the faster the pore pressure increase is, which is totally consistent with physical analysis.
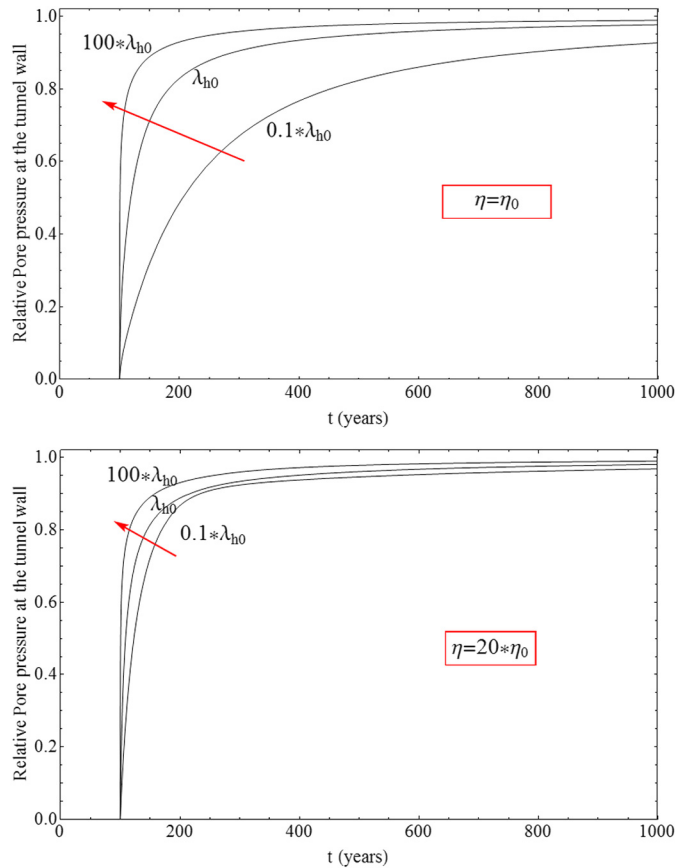
**Fig. 4.** Temporal evolution of relative pore pressure at the tunnel wall with different hydraulic conductivities and with: a) $\eta = \eta_0$; b) $\eta = 20\eta_0$.

The illustration of the pore pressure evolution is complemented by Fig. 5(a, b), where the profiles are plotted for different times. In the case of low viscosity ($\eta = \eta_0$), Fig. 5a evidences that water pressure increases with the distance from the tunnel wall and tends at far field toward its initial hydrostatic value. This is consistent with a water movement from the rock mass toward the tunnel, as discussed before. By contrast, for a higher viscosity ($\eta = 20\eta_0$), Fig. 5b shows that after backfilling ($t = 120$ and 200 years), the minimum of the water pressure is not located at the tunnel wall, but somewhere inside the rock mass. This can be interpreted by water outflowing from the cavity when creep becomes dominant, which is consistent with the converging movement of the tunnel wall after a first period of divergent displacement (Fig. 3).

Fig. 6 shows the temporal evolution of the relative convergence with different backfilling times $t_3$. Two cases are considered: $\eta = \eta_0$ and $\eta = 20\eta_0$. In the first case (dashed lines), creep stabilizes quickly (within 15 years), namely before the three considered values of $t_3$ (50, 100, and 200 years). The observed behaviours for all these values of $t_3$ are therefore similar to the divergent movements of the rock mass, tending towards the same asymptotic value at large times. This observation can be explained reminding that the constitutive model used in this study leads to a partial decoupling between mechanical and hydraulic behaviour (see Section 2). Therefore, the theoretical convergence of the tunnel for large time values only depends on the mechanical boundary condition at the tunnel wall. As the pore pressure always tends toward its initial hydrostatic value at large times, and the backfill is not loaded in this case ($\eta = \eta_0$), the mechanical boundary condition at the tunnel wall is the same for any value of $t_3$. Thus, provided that backfilling takes place after the end of creep, the same convergence is obtained for large time values whatever $t_3$: $U(\infty) = -[\frac{P_\infty}{2G(1+\frac{t_2}{T_0})} + \frac{P_\infty - p_{w0}}{K_L}]$, which gives,

for this set of parameters, $U(\infty) = 9.36 \cdot 10^{-3}$, as plotted in Fig. 6. However, it has to be underlined that the divergence of the rock mass is accompanied by an elastic discharge of the lining which, if it becomes excessive, can lead to unrealistic tensions therein because of the close contact condition assumed during Stage 4A (see § 2.1).

It should be kept in mind that the above calculation is only valid for the case where Stage 4B does not occur (the backfill is not loaded). By contrast, if the backfill is emplaced soon enough (for example when $t_3 = 50$ or 100 years when $\eta = 20\eta_0$), the divergent movement is followed by a re-convergence that loads the backfill, and the convergences are thereby lower (continuous lines).
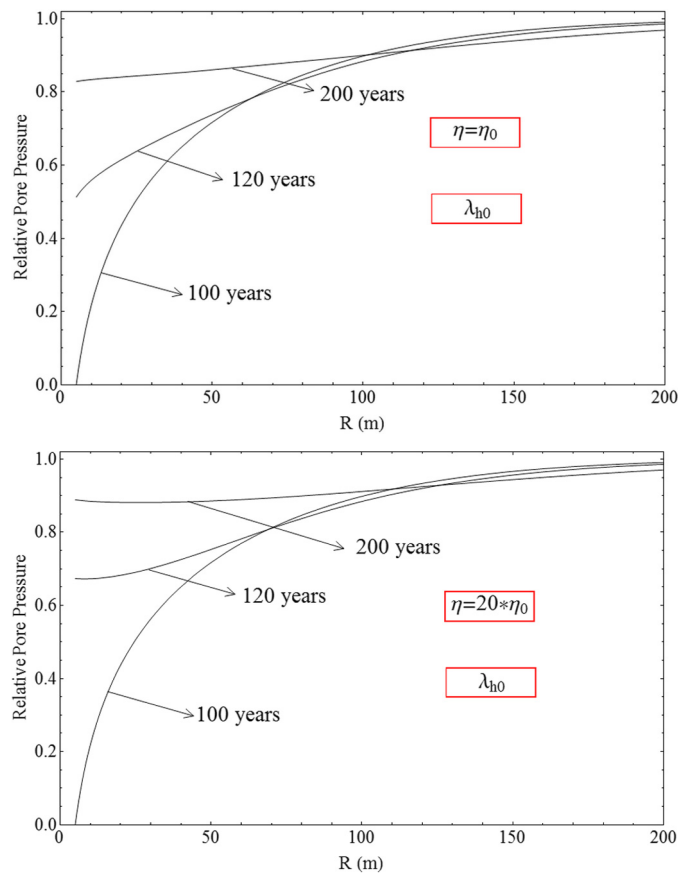
**Fig. 5.** Profiles of relative pore pressure at different times with a) $\eta = \eta_0$; b) $\eta = 20\eta_0$.
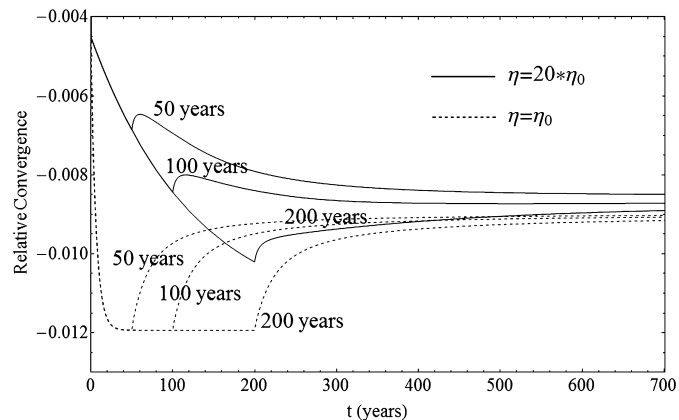


**Fig. 6.** Temporal evolution of relative convergence with different time of backfill emplacement $t_3$ (continuous lines: $\eta = 20\eta_0$; dashed lines: $\eta = \eta_0$).

## 5. Conclusions

This paper presents a semi-analytical solution for the post-closure behaviour of a typical deep tunnel drilled into a viscoplastic saturated rock mass. The main mathematical tools used in the resolution are the Laplace transform and Stehfest's algorithm. The consistency of the solution is illustrated via some numerical applications and parametric studies on the behaviour of a typical tunnel. Despite the simplifying assumptions (elastically incompressible rock mass, exponent $n = 1$ in Norton's law, creep effects slower than hydraulic flow…), it provides a useful benchmark solution for more complex numerical simulations and helps improve the physical understanding of the complex phenomena encountered during HM behaviour at the post-closure stage of such cavities.

## Appendix A. Reformulation of mechanical boundary condition

From Equations (11) and (12), we obtain the tensorial differential equation:

$$\dot{\boldsymbol{\varepsilon}} = \frac{1}{2G}\dot{\boldsymbol{s}} + \frac{3}{2\eta}\boldsymbol{s} \tag{39}$$

This, by the same procedure as in [17], provides:

$$s_z = 0$$
$$s_\theta = e^{-\frac{t}{T_0}}\left[2Gk_u - e^{\frac{t_3}{T_0}}P_\infty\left(\frac{a}{r}\right)^2 e^{-\frac{(t_3-t_2)}{T_2}}\right] \tag{40}$$
$$s_r = -e^{-\frac{t}{T_0}}\left[2Gk_u - e^{\frac{t_3}{T_0}}P_\infty\left(\frac{a}{r}\right)^2 e^{-\frac{(t_3-t_2)}{T_2}}\right]$$

where $k_u = \frac{a^2}{r^2}\int_{t_3}^t e^{\frac{t'}{T_0}}\dot{U}(t')dt'$. Note that we can express equivalently $s_r = g(t)\frac{a^2}{r^2}$ with $g(t) = e^{-\frac{t}{T_0}}[-2G\int_{t_3}^t e^{\frac{t'}{T_0}}\dot{U}(t')dt' + e^{\frac{t_3}{T_0}}P_\infty e^{-\frac{(t_3-t_2)}{T_2}}]$. The substitution of (40) in (3) leads, on account of the boundary condition at far field, to the following expression of the radial stress:

$$\sigma_r = \frac{a^2}{r^2}g(t) - P_\infty \tag{41}$$

Substituting (41) into the boundary condition (19), we get:

$$-2G\int_{t_3}^t e^{\frac{t'}{T_0}}\dot{U}(t')dt' + e^{\frac{t_3}{T_0}}P_\infty e^{-\frac{(t_3-t_2)}{T_2}} = e^{\frac{t}{T_0}}\left[P_\infty + K_L(U - U_2) - p_w(a,t)\right] \tag{42}$$

Taking the time derivative of (42) allows us to reformulate the mechanical boundary condition as follows:

$$\dot{U}(t) + \frac{1}{T_2}U(t) = \frac{K_L U_2 + p_w(a,t) - P_\infty}{K_L T_2} + \frac{\dot{p_w}(a,t)}{K_L + 2G} \tag{43}$$

## Appendix B. Exact solution for the case of a dry compressible ground, $\nu \neq 0.5$

In this case, no hydraulic effect occurs, thus rock mass and lining continue to move towards the tunnel and compress the backfill due to the creep effect. The mechanical boundary condition at the tunnel wall writes:

$$\sigma_r(a,t) = -\left[p_L(t) + p_R(t)\right] = K_L\left[U(t) - U_2\right] + K_R\left[U(t) - U_3\right] \tag{44}$$

In this case, the hypothesis of elastic incompressibility is not made. Contrariwise, the assumption $n = 1$ is still needed. The resolution procedure is similar to the one described in [17]. The key steps are recalled here. From (5) and (13), combining with the boundary condition at far field, we get:

$$\dot{\sigma}_m = K\dot{\epsilon}; \qquad \sigma_m = K\epsilon - P_\infty \tag{45}$$

The combination of (5), (13) and (45) imply:

$$\dot{\boldsymbol{\varepsilon}} = \frac{1}{3}\dot{\epsilon}\mathbf{1} + \frac{1}{2G}\dot{\boldsymbol{s}} + \frac{3}{2\eta}\boldsymbol{s} \tag{46}$$

which, by the same reasoning as in [17], provides:

$$s_z = -\frac{2G}{3}e^{-\frac{t}{T_0}}k_\epsilon^*$$
$$s_\theta = e^{-\frac{t}{T_0}}\left[2G\left(k_u^* - \frac{1}{3}k_\epsilon^*\right) - e^{\frac{t_3}{T_0} - \frac{(t_3-t_2)}{T_2}}P_\infty\left(\frac{a}{r}\right)^2\right] \tag{47}$$
$$s_r = e^{-\frac{t}{T_0}}\left[2G\left(\frac{2}{3}k_\epsilon^* - k_u^*\right) + e^{\frac{t_3}{T_0} - \frac{(t_3-t_2)}{T_2}}P_\infty\left(\frac{a}{r}\right)^2\right]$$

where $k_\epsilon^* = \int_{t_3}^t e^{\frac{t'}{T_0}}\dot{\epsilon}(r,t')dt'$ and $k_u^* = \frac{1}{r}\int_{t_3}^t e^{\frac{t'}{T_0}}\dot{u}(r,t')dt'$. Substituting (45) and (47) into (3), then taking the time derivative of the obtained equation, we get: $(K + \frac{4G}{3})\partial_r\dot{\epsilon}(r,t) + \frac{K}{T_0}\partial_r\epsilon(r,t) = 0$. Invoking the boundary condition at infinity, the last equation leads to:

$$\frac{\partial \epsilon(r,t)}{\partial t} + \frac{\epsilon(r,t)}{T_1} = 0 \tag{48}$$

where $T_1 = (K + 4G)T_0/K$ is the characteristic time of creep. Accounting for the initial conditions of zero strains, the solution of (48) writes:

$$\epsilon(r,t) = 0 \tag{49}$$

One can realize that although $\nu \neq 0.5$, the milieu is still isochoric and thereby (13) is still valid. Substituting (49) in (47) and expressing the radial total stress at the tunnel wall $s_r$

$$\left[ \frac{-2G}{a} \int_{t_3}^{t} e^{\frac{t'}{T_0}} \dot{u}(a,t') dt' + e^{\frac{t_3}{T_0} - \frac{(t_3-t_2)}{T_2}} P_\infty \right] - e^{\frac{t}{T_0}} P_\infty = e^{\frac{t}{T_0}} \left[ (K_L + K_R)U(t) - K_L U_2 - K_R U_3 \right] \tag{50}$$

Taking the time derivative of (50), we obtain:

$$\dot{U}(t) + \frac{1}{T_3}U(t) = \frac{K_L U_2 + K_R U_3 - P_\infty}{(K_L + K_R)T_3} \tag{51}$$

of which the solution, by accounting for the initial condition at this stage, writes:

$$U(t) = U_3 - \frac{P_\infty}{K_L + K_R} e^{-\frac{t_3-t_2}{T_2}} \left( 1 - e^{-\frac{t-t_3}{T_3}} \right) \tag{52}$$

Comparing this result with the one in Stage 3 (Table 1), we can see that the presence of the backfill slows down the convergence rate. Explicit expressions for stresses are then deduced:

$$\sigma_r = -P_\infty \left[ 1 - \left( \frac{a}{r} \right)^2 e^{-\frac{(t-t_3)}{T_3} - \frac{(t_3-t_2)}{T_2}} \right]$$
$$\sigma_\theta = -P_\infty \left[ 1 + \left( \frac{a}{r} \right)^2 e^{-\frac{(t-t_3)}{T_3} - \frac{(t_3-t_2)}{T_2}} \right] \tag{53}$$
$$\sigma_z(r,t) = -P_\infty$$

## References

[1] A. Afrouz, Methods to reduce floor heave and sides closure along the arched gate roads, Min. Sci. Technol. 10 (3) (1990) 253–263.
[2] P. Bérest, J. Bergues, B. Brouard, J. Durup, B. Guerber, A salt cavern abandonment test, Int. J. Rock Mech. Min. Sci. 38 (2001) 357–368.
[3] P. Cosenza, M. Ghoreychi, Effects of very low permeability on the long-term evolution of a storage cavern in rock salt, Int. J. Rock Mech. Min. Sci. 36 (1999) 527–533.
[4] H. Wong, M. Morvan, F. Deleruyelle, C.J. Leo, Analytical study of mine closure behaviour in a poro-elastic media, Comput. Geotech. 35 (2008) 645–654.
[5] J.A. Hudson, O. Stephansson, J. Andersson, C.F. Tsang, L. Jing, Coupled T–H–M issues relating to radioactive waste repository design and performance, Int. J. Rock Mech. Min. Sci. 38 (1) (2001) 143–161.
[6] L. Liedtke, W. Bleich, Convergence calculations for back-filled tunnels in rock salt, Comput. Struct. 21 (1/2) (1985) 353–378.
[7] M. Chijimatsu, T. Nguyen, L. Jing, J. De Jonge, M. Kohlmeier, A. Millard, A. Rejeb, J. Rutqvist, M. Souley, Y. Sujita, Numerical study of the THM effects on the near-field safety of a hypothetical nuclear waste repository—BMT1 of the DECOVALEX III project. Part 1: Conceptualization and characterization of the problems and summary of results, Int. J. Rock Mech. Min. Sci. 42 (2005) 720–730.
[8] J. Rutqvist, A. Backstrom, M. Chijimatsu, X. Feng, P. Pan, J. Hudson, L. Jing, A. Kobayashi, T. Koyama, H. Lee, X. Huang, B. Rinne, B. Shen, A multiple-code simulation study of the long-term EDZ evolution of geological nuclear waste repositories, Environ. Geol. 57 (6) (2009) 1313–1324.
[9] H. Wong, M. Morvan, F. Deleruyelle, C.J. Leo, Analytical study of mine closure behaviour in a poro-visco-elastic medium, Int. J. Numer. Anal. Methods Geomech. 32 (14) (2008) 1737–1761.
[10] N. Dufour, H. Wong, F. Deleruyelle, C. Leo, Hydromechanical post-closure behaviour of a deep tunnel taking into account a simplified life cycle, Int. J. Geomater. 12 (5) (2012) 1–11.
[11] M. Gasc-Barbier, S. Chanchole, P. Berest, Creep behavior of Bure clayey rock, Appl. Clay Sci. 26 (2004) 449–458.
[12] A. Giraud, G. Rousset, Time-dependent behaviour of deep clays, Eng. Geol. 41 (1996) 181–195.
[13] C. Zhang, T. Rothfuchs, Experimental study of the hydro-mechanical behaviour of the Callovo–Oxfordian argillite, Appl. Clay Sci. 26 (2004) 325–336.
[14] T. Bui, H. Wong, F. Deleruyelle, A. Zhou, X. Lei, A coupled poroplastic damage model accounting for cracking effects on both hydraulic and mechanical properties of unsaturated media, Int. J. Numer. Anal. Methods Geomech. 40 (5) (2016) 625–650.
[15] C. Tsang, J. Barnichon, J. Birkholzer, X. Li, X. Xillen, Coupled thermo-hydro-mechanical processes in the near field of a high-level radioactive waste repository in clay formations, Int. J. Rock Mech. Min. Sci. 49 (2012) 31–44.
[16] T. Bui, H. Wong, F. Deleruyelle, A. Zhou, Constitutive modelling of the time-dependent behaviour of partially saturated rocks, Comput. Geotech. 78 (2016) 123–133, http://dx.doi.org/10.1016/j.compgeo.2016.05.004.
[17] F. Deleruyelle, T. Bui, H. Wong, N. Dufour, Analytical modelling of a deep tunnel in a viscoplastic rock mass accounting for a simplified life cycle and extension to a particular case of porous media, in: Special Publications Clays in Natural and Engineered Barriers for Radioactive Waste, vol. 400, Geological Society, London, 2014.
[18] O. Coussy, Poromechanics, John Wiley Sons LTD, Chichester, UK, 2004.
[19] H. Stehfest, Algoritm 368: numerical inversion of Laplace transform, Commun. ACM 13 (1) (1970) 47–49.
[20] J. Lemaitre, J. Chaboche, Mechanics of Solid Materials, Cambridge University Press, Cambridge, 1990.
[21] T. Bui, H. Wong, F. Deleruyelle, N. Dufour, C. Leo, D. Sun, Analytical modeling of a deep tunnel inside a poro-viscoplastic rock mass accounting for different stages of its life cycle, Comput. Geotech. 58 (2014) 88–100.

[22] ANDRA, Stockage réversible profond, étape 2009, ANDRA, Paris, 2009.

[23] Y. Wileveau, F. Bernier, Similarities in the hydromechanical response of Callovo–Oxfordian clay and Boom Clay during gallery excavation, Phys. Chem. Earth 33 (2008) S343–S349.

[24] M. Panet, Le calcul des tunnels par la méthode convergence–confinement, Presses de l'École nationale des ponts et chaussées, Paris, 1995.

[25] V. Nguyen, Couplage dégradation chimique—comportement en compression du béton, Thèse de doctorat, École nationale des ponts et chaussées, Paris, 2005.